

Infiltrating Semiconducting Polymers into Self-Assembled Mesoporous Titania Films for Photovoltaic Applications**

By Kevin M. Coakley, Yuxiang Liu, Michael D. McGehee,* Karen L. Frindell, and Galen D. Stucky

Interpenetrating networks of organic and inorganic semiconductors are attractive for photovoltaic cells because electron transfer between the two semiconductors splits excitons. In this paper we show that films of titania with a uniform distribution of pore sizes can be made using a block copolymer as a structure-directing agent, and that 33 % of the total volume of the film can be filled with a semiconducting polymer.

1. Introduction

A promising approach for making inexpensive photovoltaic cells is to fill nanoporous titania films with organic semiconductors.^[1–7] When the organic semiconductor or a sensitizing dye adsorbed on the titania surface absorbs light, electron transfer to the titania takes place before the photogenerated electrons and holes recombine. The electrons then travel through the titania to an electrode on one side of the film and the holes travel through the organic semiconductor to an electrode at the other side of the film. The titania film is usually made by doctor blading a paste of titania nanocrystals and then sintering them together. The organic semiconductor is typically incorporated into the pores by spin casting. Although there have been several reports on photovoltaic cells made in this way, there have been no studies that show how well the organic semiconductor infiltrates the pores of the titania film. Since polymers suffer a loss of conformational entropy when they are confined in a channel whose radius is less than their radius of gyration, filling the pores with a polymer has been thought to be a challenge.

In this contribution we describe a method for making titania films that have a more optimal pore structure than that of sintered titania nanoparticle films. The films are made by dip

coating substrates with a solution of a titania sol–gel precursor and a structure-directing block copolymer. After the precursor and block copolymer co-assemble into an ordered mesostructure, the block copolymer is removed as the films are calcined at temperatures in the range of 400–450 °C. The pore size, titania wall thickness, and film thickness are all extremely uniform. We have not yet optimized these parameters for photovoltaic applications, but the potential to do so exists. We also describe here a technique for incorporating the semiconducting polymer regioregular poly(3-hexyl thiophene) (RR P3HT) into the titania pores by spin casting a film of the polymer on top of the titania film, and then heating at temperatures in the range of 100–200 °C. We used RR P3HT in these experiments because it has a hole mobility of $0.1 \text{ cm}^2 \text{ V}^{-1} \text{ s}^{-1}$ in field-effect transistors and a relatively small bandgap. Depth-profiling experiments with an X-ray photoelectron spectrometer (XPS) show that the polymer penetrates all the way to the bottom of the titania films. UV-vis and photoluminescence (PL) spectroscopy measurements show that the RR P3HT chains are more coiled inside the mesoporous titania than they are in a semicrystalline spin cast film. The PL measurements also show that most of the excitons in the polymer are quenched, which suggests that electron transfer from the polymer to the titania occurs. Our approach for making organic–inorganic nanostructures should not only yield photovoltaic cells with enhanced efficiency, but will also enable direct transport measurements of polymer chains confined in nanopores.

2. Results and Discussion

Although there have been many reports of synthesizing well-ordered silica mesostructures in powder^[8–11] and thin-film form^[12,13] using organic structure-directing agents, there have been relatively few descriptions of titania mesostructures until recently.^[14–23] Mesostructure synthesis with titania sol–gel precursors is more challenging because the rates of hydrolysis and condensation tend to be much faster. If these rates are too fast, large particles of titania form before mesostructures have a chance to self-assemble. If water is removed from the synthesis to slow down hydrolysis and condensation, it is difficult to con-

[*] Prof. M. D. McGehee, K. Coakley
Department of Materials Science and Engineering
Stanford University
Stanford, CA 94305-2205 (USA)
E-mail: mmcgehee@stanford.edu

Y. Liu
Department of Chemistry
Stanford University
Stanford, CA 94305 (USA)

K. Frindell, Prof. G. D. Stucky
Department of Chemistry
University of California at Santa Barbara
Santa Barbara, CA 93106 (USA)

[**] We acknowledge the Camille and Henry Dreyfus Foundation, the Petroleum Research Fund and the U.S. National Science Foundation (DMR-96-34396 and NSF CHE 0098240) for support of this research. This work was also partially supported by the NSF-MRSEC program through the Center on Polymer Interfaces and Macromolecular Assemblies (CPIMA) under DMR 9808677. We thank Dr. Ekaterina Kadnikova for making GPC measurements and Ann Marshall for HR SEM assistance.

control the rate of hydrolysis, which then occurs as a result of ambient water. Recently it has been shown that titania mesostructures with lamellar, hexagonal and cubic symmetries can be made using titanium(IV) tetraethoxide (TEOT) as the titania precursor and a Pluronic poly(ethylene oxide)–poly(propylene oxide)–poly(ethylene oxide) tri-block copolymer (P123) as the structure-directing agent.^[11,17,24] We have used this procedure to make the films described in this manuscript. A key feature of the synthesis is to mix the TEOT with concentrated hydrochloric acid to prevent rapid condensation of the titania precursors. The first step in the synthesis is to mix the acidic solution of TEOT with a solution of the P123 in ethanol. A mesostructure does not form at this point because the precursors are too dilute. After the solution has been aged to allow a small degree of condensation of the titania precursor, thin films are deposited by dip coating. Mesostructure self-assembly takes place as the ethanol evaporates from the thin film. The structural phase of the pores in the mesostructure is determined by the temperature and the volume fraction of titania to block copolymer. After the films have dried, the titania precursors remain uncondensed until heat treatment takes place. As the films are heated at a rate of 1 °C min⁻¹, the titania condenses to form a rigid network. At approximately 270 °C, the block copolymer oxidizes and leaves the pores. At higher temperatures the amorphous titania partially crystallizes to form a semicrystalline network. Calcined films are transparent and have essentially no cracks or defects that can be observed with an optical microscope. The final film thickness can be varied between 50 and 300 nm by controlling the amount of ethanol that is used to dilute the precursor mixture.

Since a pore system that runs from the top of the film to the bottom is needed for photovoltaic applications and for rapid polymer infiltration, we chose to use synthesis conditions that yield a three-dimensional cubic pore structure for the studies shown here. All films were made on indium tin oxide (ITO)-coated glass substrates. Figure 1 shows the X-ray diffraction (XRD) pattern taken from a mesostructured sample before and after the block copolymer was removed by heating to 400 °C. Since there is only one diffraction peak, we conclude that the films have short-range order, but not a high degree of long-range order. While it is not possible to determine the symmetry of the pore structure in the film with just one diffraction peak, we think that the peak can be assigned to the (200) planes of a film having *Im* $\bar{3}m$ cubic symmetry because of previous XRD and transmission electron microscopy (TEM) studies on more highly ordered mesoporous titania and silica samples.^[11,24] The diffraction data in Figure 1 shows that during heating at 400 °C, the periodicity of the titania film shrank from 26 nm to 13 nm in the direction normal to the film. The film shrinkage is primarily a result of the condensation and partial crystallization of the titania network during heating. Calcination at 425 °C and 450 °C further reduced the titania periodicity to 11.8 nm and 9.5 nm, respectively.

Figure 1 also shows a high-resolution scanning electron microscopy (HRSEM) image of the top surface of a calcined mesoporous titania film. Although the degree of long-range order is not very high, the image clearly shows that the pore network

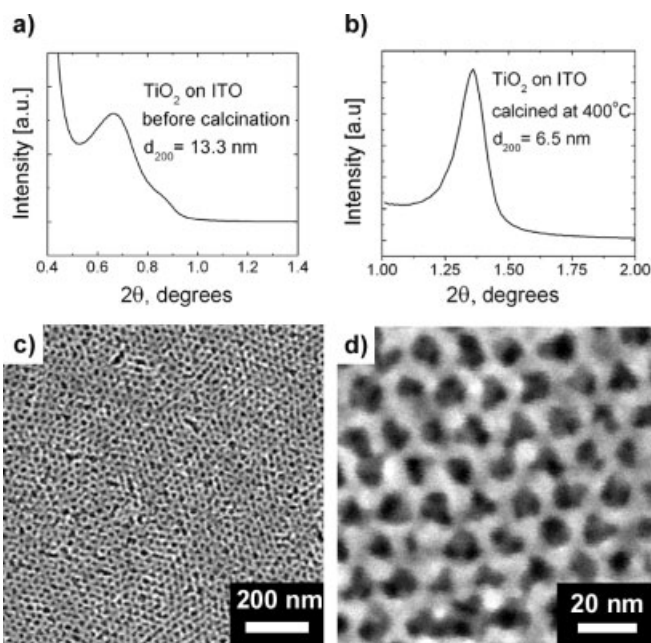


Fig. 1. Mesoporous titania characterization. X-ray diffraction patterns of mesoporous titania before (a) and after (b) calcination at 400 °C, and HRSEM images of calcined mesoporous titania at two different magnifications (c,d). Pores with 3-fold rotational symmetry are shown in (d).

is accessible from the surface of the film and that the pore size is very uniform. The pores in the higher magnification image in the figure appear to be oriented along the (111) zone axis. We suspect that the top surface has a different orientation than the rest of the film because of interactions with the air interface. The SEM image also shows that the pores on the surface are approximately 10 nm in diameter in the plane of the film. Considering both the XRD and HRSEM results, we conclude that the pore structure of the titania films consists of a connected network of ellipsoidally shaped holes with a 10 nm diameter in the plane of the film and a 4–6 nm diameter in the direction normal to the film. The asymmetry in the pore shape arises because most of the shrinkage during calcination occurs in the direction normal to the substrate.

Others have infiltrated semiconducting polymers into nanoporous materials by placing the materials in contact with a liquid solution of the polymer, either by spin-casting^[3,5,6] or direct submersion.^[25,26] We chose to fill the mesoporous films by heating them in direct contact with a solid film of the polymer. Conjugated polymer films of RR P3HT were first spin-cast on top of mesoporous films, and then the samples were heated for various times and temperatures. Following heat treatment, the excess polymer that did not infiltrate the mesoporous films was removed by rinsing the samples in toluene. Using UV-vis absorption measurements, we observed that the amount of polymer remaining in the sample stabilized after 5–10 min of rinsing and then remained constant. By contrast, heat-treated polymer residing on top of bare ITO or glass was found to dissolve very quickly in toluene. These observations provide indirect evidence that polymer penetrates into the pores during the heating and show that the polymer stays in the pores even if the film is rinsed in a good solvent.

We performed XPS depth profiling to prove directly that RR P3HT infiltrated the pores of mesoporous titania. This technique allows the measurement of elemental concentrations as a film sample is slowly sputtered away. The results of this experiment are shown in Figure 2 for samples heated for 4 h at 200 °C and 16 h at 100 °C. Depth profiling of a mesoporous film with no embedded conjugated polymer showed only trace

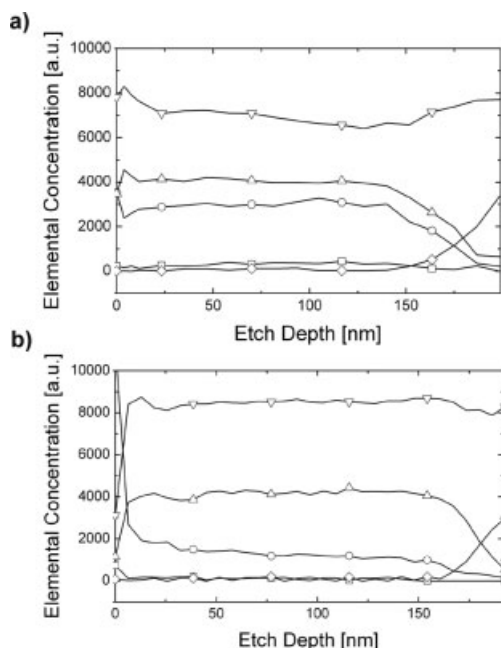


Fig. 2. XPS depth profiling of RR P3HT/mesoporous titania samples after a) 4 h at 200 °C and b) 16 h at 100 °C. The peaks used to detect elemental concentration were oxygen 1s (inverted triangles), titanium 2p (triangles), carbon 1s (circles), sulfur 2p (squares), and indium 3d (diamonds).

carbon signals. Hence the carbon signal observed in the two samples in Figure 2 is entirely attributable to the embedded RR P3HT. Both sets of data clearly show that the polymer penetrates to the bottom of the films and that there is only a small amount of polymer on the surface of the film that is not inside the pores.

The M_n and polydispersity of the RR P3HT were 20 000 g mol⁻¹ and 2.0, respectively. The radius of gyration of the chains is probably in the range of 6–9 nm.^[27] Since the polymer chains have a radius of gyration that is larger than the semi-axes of the ellipsoidal pores of the titania, it is likely that there is a conformational entropy loss associated with infiltration. We propose that this entropy loss is compensated by a strong enthalpic interaction between the highly polarizable main chain of the RR P3HT and the polar titania, and that a chain of RR P3HT will infiltrate only if some of its segments are able to adsorb on the walls of the titania. This is analogous to the intercalation of polymer melts in layered silicates, in which a favorable enthalpic interaction allows the polymer chains to penetrate into nanometer-sized galleries.^[28,29]

The rate and temperature dependence of infiltration was measured by heating RR P3HT/titania samples for varying periods of time and then measuring the embedded RR P3HT optical density after the remaining uninfiltreated polymer had

been rinsed off. Figure 3 shows the optical density that resulted from infiltrating polymer at several different temperatures for varying amounts of time. We chose to use temperatures well

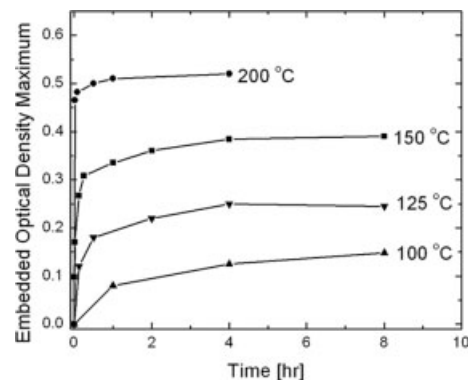


Fig. 3. Optical density of embedded RR P3HT after infiltration for varying periods of time at the indicated temperatures.

above the glass-transition temperature of the polymer, which we measured to be 25 °C using differential scanning calorimetry (DSC). At 200 °C, the optical density of embedded polymer reached 0.5 after just a few minutes of heating. Since a pure film of polymer would have to be 60 nm thick to have this optical density, and since we expect that the ability of the chains to absorb light is not significantly changed by putting them in the pores, we estimate that 33 % of the total volume of the 180 nm thick mesoporous film was occupied by RR P3HT. At lower temperatures the rate of infiltration was slower and the volume of infiltrated polymer was less, even if long infiltration times were used. For example, at 100 °C it took approximately 20 h for the optical density of embedded polymer to saturate. The final optical density was only 0.2.

There are several possible reasons that less polymer infiltrates the films at lower temperatures. We rule out the possibility that the polymer did not reach the bottom of the mesoporous film at 100 °C because of the depth-profiling data shown in Figure 2. One possible explanation is that the polymer reached the bottom in some pore channels, but did not penetrate other pore channels at all. We consider this unlikely because the SEM images show that the pore size distribution on the sample surface is uniform. Furthermore, the film has a three-dimensional interconnected network of pores. Even if some regions of a pore channel were clogged, the polymer could probably get around the clogs and fill the rest of the channel. Another possibility is that the titania walls could have adsorbed water or solvent molecules on their surface even though they were taken directly from a furnace to a nitrogen glove box before the polymer was deposited. These molecules could limit the amount of polymer that can be infiltrated. Increased infiltration at high temperatures could be a result of increased desorption of water or solvent molecules. The most likely explanation is that the polymer chains form a thicker coating on the titania at higher temperatures. It is known that as RR P3HT in a neat film is heated from 100 °C to 200 °C its π -stacked crystals break up and take on an increasingly coiled structure.^[30] Inside the mesopores, coiled chains occupy a

smaller titania surface area than rod-like chains. Consequently, a greater number of chains can be adsorbed on the titania surface at high temperatures.

Insight on the RR P3HT chain configuration inside the pores can be gleaned from the absorption spectra of the embedded polymers after infiltration. The absorption spectrum of a RR P3HT chain in a coiled configuration is blue-shifted relative to the spectrum of a rod-like chain because the conjugation length is shorter on a coiled chain.^[30–33] Figure 4 shows the normalized absorption spectra of samples that have been heated for

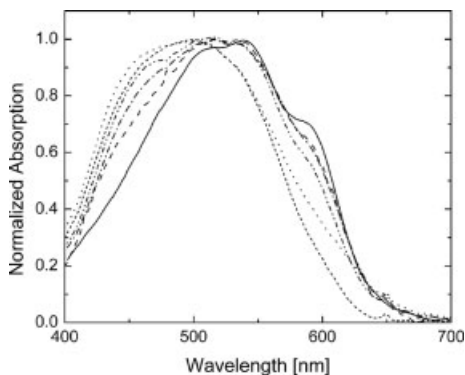


Fig. 4. Room-temperature RR P3HT absorption spectra following infiltration for 4 h at different temperatures. Increasing blue-shifts correspond to increasing temperatures. The temperatures used were 100 °C (dash), 125 °C (dash dot), 150 °C (dash dot dot), 165 °C (dot), and 200 °C (short dash). For comparison a neat RR P3HT film was also heated for 4 h at 200 °C (solid line).

4 h at different temperatures and then cooled to room temperature. For comparison, the spectrum of a neat polymer film that has been treated for 4 h at 200 °C and then cooled is also shown. The neat film had nearly identical spectra before and after heating. For the chains that have been infiltrated into mesoporous titania the absorption spectra were blue-shifted. This suggests that some RR P3HT chain segments remain locked in a coiled configuration and are unable to crystallize following infiltration at high temperatures.

The emission spectra of conjugated polymers can also be used to obtain information about the polymer chain morphology. In a pure film of RR P3HT, the peak of the emission spectrum is red-shifted from the peak of the absorption spectrum by 180 nm (0.58 eV). The shift is larger than for most conjugated polymers because the chains of RR P3HT have a tendency to crystallize, which results in a high degree of π - π stacking that enables excitons to delocalize over more than one chain.^[34] Figure 5 shows the measured photoluminescence (PL) spectra from RR P3HT embedded in mesoporous titania after heating for 4 h at different temperatures, and from a control sample of pure polymer that was heated for 4 h at 200 °C. As Figure 5 shows, the emission spectrum of the polymer when it is in the mesoporous titania is not as red-shifted as it is in a neat film, suggesting that the excitons on the polymer chains in the pores are less able to delocalize. This data gives additional evidence that the polymer chains do not π -stack to a significant extent inside the pores.

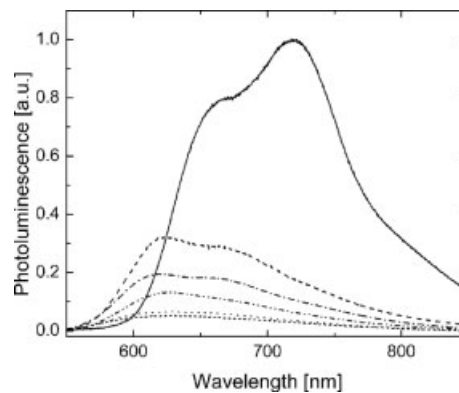


Fig. 5. Photoluminescence spectra from RR P3HT after infiltration for 4 h at different temperatures. Higher infiltration temperatures correspond to increased photoluminescence. The temperatures used were 200 °C (dash), 175 °C (dash dot), 150 °C (dash dot dot), 125 °C (dot), and 100 °C (short dash). For comparison a neat RR P3HT film was also heated for 4 h at 200 °C (solid line).

Photoluminescence measurements can also be used to determine the effectiveness of photoinduced charge transfer from the polymer to the titania.^[35,36] The PL spectra shown in Figure 5 were calculated by dividing the measured PL spectra by the number of photons absorbed. Consequently, the relative quantum yields of each film can be determined by comparing the integrated area under each curve. Table 1 shows the approximate quenching efficiencies, defined as $1 - (\text{embedded film PL} / \text{neat film PL})$, for each of the samples. One might expect that there would be a negligible amount of luminescence from

Table 1. Approximate photoluminescence quenching efficiencies for RR P3HT infiltrated into mesoporous titania for 4 h at different temperatures.

Temperature [°C]	125	150	165	175	200
Quenching efficiency [%]	94.8	93.4	87.1	80.4	67.6

the RR P3HT when it is in the mesoporous titania since it is known that charge transfer usually occurs with a very high efficiency if excitons are formed within approximately 10–20 nm of a titania interface.^[37] One possible reason that the luminescence is higher than expected is that the polymer chains do not aggregate inside the pores. Consequently, the PL efficiency of the chains in the pores would probably be higher than in a neat film if electron transfer did not occur. Nonetheless, it is clear that some of the excitons are not able to diffuse to the titania interface and donate an electron to the titania, even though they are formed within a few nanometers of the interface. Table 1 shows that the quenching efficiency decreases as the temperature used to infiltrate the polymers increases. There are several factors that can explain this trend. The first is that exciton diffusion is hindered by poor coupling between the polymer chains, which are probably more coiled when they are infiltrated at higher temperatures. The second is that the polymer coatings are thicker when they are formed at higher temperatures. Consequently, excitons in these films can be formed farther from the titania interface. A third factor is that the hex-

yl side chains might act as a barrier between the conjugated backbone and the titania interface. The infiltration temperature might affect the way that the polymer chains attach to the titania and thereby affect the quenching efficiency. Further experiments will be needed to understand the processes of exciton diffusion and electron transfer in these films.

3. Conclusions

In conclusion, we have made an interpenetrating semiconductor nanostructure by infiltrating RR P3HT into mesoporous titania films with uniformly sized pores. The amount of polymer that can be incorporated into the films depends on the temperature that is used for infiltration. At 200 °C it is possible to achieve an optical density of 0.5 by infiltrating RR P3HT into a 180 nm titania film in less than 1 h. XPS depth profiling data and UV-vis absorption measurements show unequivocally that the polymer infiltrates uniformly to the bottom of the film and are consistent with a model that the polymer adsorbs on the walls of the titania. Both UV-vis absorption and PL measurements indicate that the chains of the RR P3HT are coiled and unable to efficiently π -stack inside the pores of the titania. For this reason, we suspect that the mobility for charge carriers in the polymer is probably much less than $10^{-1} \text{ cm}^2 \text{ V}^{-1} \text{ s}^{-1}$, which is the field-effect mobility of high-quality thin films of RR P3HT. The PL measurements also suggest that electron transfer from the polymer to the titania occurs, but that it does not occur 100 % of the time. Exciton diffusion is probably hindered by less than ideal polymer chain packing. It should be possible to improve the efficiency of electron transfer and the charge carrier mobility by modifying the films in such a way that the polymer chains stack more directly on each other. With the films we have made and similar ones made with silica instead of titania, it is possible to perform direct charge transport measurements on semiconducting polymers that are confined to nanometer-sized channels. We will report on these measurements and the fabrication of photovoltaic cells in a separate manuscript.

4. Experimental

To make mesoporous titania films, we first mixed 3.2 g concentrated HCl with 4.3 g titanium ethoxide. 1 g Pluronic P123 and 10–20 g ethanol were then stirred into the solution. Both the titanium ethoxide and Pluronic P123 were obtained from Aldrich and used without further purification. After approximately 10 min of stirring, ITO-coated glass substrates were dip coated using a coating speed of 6 cm min^{-1} . The samples were subsequently aged at 13 °C for 48 h, and then calcined using a heating rate of $1 \text{ }^\circ\text{C min}^{-1}$ to 450 °C to remove the block copolymer and densify the titania. Final titania film thickness was measured with a Dektak profilometer. X-ray diffraction patterns were recorded on a Philips Materials Research Diffractometer in parallel beam mode using $\text{Cu K}\alpha$ radiation. High-resolution SEM images were taken using a FEI Sirion field-emission SEM with an accelerating voltage of 5.0 kV.

P3HT, obtained from Aldrich, was purified in a nitrogen atmosphere by Soxhlet extraction with hexane and chloroform, followed by the removal of the chloroform under vacuum. The final product was dried at 45 °C in vacuum for 24 h. All polymers and their solutions were stored inside a glove box filled with nitrogen to prevent degradation and oxidation. Differential scanning calorimetry (DSC) measurements were performed on a Perkin-Elmer DSC-7 calibrated with indium. The polymer sample was first heated to 280 °C and then cooled down to

–30 °C at $40 \text{ }^\circ\text{C min}^{-1}$ to remove its thermal history. All of the subsequent analyses were performed at a fixed heating and cooling rate of $40 \text{ }^\circ\text{C min}^{-1}$.

After the titania films were calcined, they were taken immediately into a nitrogen glove box. Overlying films of P3HT were spin coated on top of the mesoporous titania from a chloroform solution. The polymer layer thickness was chosen to be equal to or greater than the thickness of the underlying titania layer. This ensured that the infiltration of polymer was not limited by the depletion of the polymer overlayer. We heated the samples on a hot plate at temperatures ranging from 100 °C to 200 °C and times ranging from 1 min to 48 h. After heating, the samples were removed from the glove box and rinsed in toluene to remove the remaining uninfiltated P3HT.

Depth-profiling experiments were performed with a SSI S-Probe Monochromatized XPS Spectrometer. X-rays were generated using $\text{Al K}\alpha$ radiation (1486 eV). Sample etching was performed in situ using a Leybold Heraeus argon ion etcher with a 1 mA emission current. The etch crater was $2 \text{ mm} \times 2 \text{ mm}$ in size. In order to prevent edge sampling during elemental analysis, an X-ray spot size of approximately $250 \text{ }\mu\text{m} \times 700 \text{ }\mu\text{m}$ was used. Measurement of the presence of different elements was made after each etch step by integrating the appropriate elemental peak area. Each integrated peak area was then divided by the sensing time and corresponding elemental sensitivity factor to give the final elemental concentration. Rotation of the sample during etching did not affect the results of the depth profiling experiments.

Absorption spectra were measured with an Ocean Optics USB2000 absorption spectrometer. Because sample reflection varied significantly in going from P3HT-filled mesoporous films to blank (unfilled) mesoporous films, the reflection spectrum of each sample was measured independently using a bifurcated Ocean Optics R series reflection probe. In this case, a mirror with a known reflection spectrum was used as a reference. We calculated the final absorption spectra using the formula $\text{OD} = -\log_{10}(T+R)$, OD: optical density, T : transmittance, R : surface reflectance. Scattering from the films was negligible. Photoluminescence measurements were made using an Acton Research Spectrapro 500i 500 mm monochromator with a charge-coupled device (CCD) array detection system and a helium cadmium laser that emits at 442 nm.

Received: November 20, 2002
Final version: February 11, 2003

- [1] U. Bach, D. Lupo, P. Comte, J. E. Moser, F. Weissortel, J. Salbeck, H. Spreitzer, M. Gratzel, *Nature* **1998**, *395*, 583.
- [2] J. Kruger, R. Plass, L. Cevey, M. Piccirelli, M. Gratzel, *Appl. Phys. Lett.* **2001**, *79*, 2085.
- [3] A. C. Arango, S. A. Carter, P. J. Brock, *Appl. Phys. Lett.* **1999**, *74*, 1698.
- [4] J. S. Salafsky, *Phys. Rev. B* **1999**, *59*, 10885.
- [5] A. J. Breeze, Z. Schlesinger, S. A. Carter, P. J. Brock, *Phys. Rev. B* **2001**, *64*, 1252051.
- [6] S. Spiekermann, G. Smestad, J. Kowalik, L. M. Tolbert, M. Gratzel, *Synth. Met.* **2001**, *121*, 1603.
- [7] D. Gebeyehu, C. J. Brabec, N. S. Sariciftci, D. Vanmaekelbergh, R. Kiebooms, F. Vanderzande, H. Schindler, *Synth. Met.* **2002**, *125*, 279.
- [8] J. S. Beck, J. C. Vartuli, W. J. Roth, M. E. Leonowicz, C. T. Kresge, K. D. Schmitt, C. T.-W. Chu, D. H. Olson, E. W. Sheppard, S. B. McCullen, J. B. Higgins, J. L. Schlenker, *J. Am. Chem. Soc.* **1992**, *114*, 10834.
- [9] D. Zhao, J. Feng, Q. Huo, N. Melosh, G. H. Fredrickson, B. F. Chmelka, G. D. Stucky, *Science* **1998**, *279*, 548.
- [10] D. Zhao, P. Yang, Q. Huo, B. Chmelka, G. D. Stucky, *Curr. Opin. Solid State Mater. Sci.* **1998**, *3*, 111.
- [11] Y. Sakamoto, M. Kaneda, O. Terasaki, D. Y. Zhao, J. M. Kim, G. D. Stucky, H. J. Shin, R. Ryoo, *Nature* **2000**, *408*, 449.
- [12] Y. Lu, R. Ganguli, C. A. Drewien, M. T. Anderson, C. J. Brinker, W. Gong, Y. Guo, H. Soye, B. Dunn, M. H. Huang, J. I. Zink, *Nature* **1997**, *389*, 364.
- [13] D. Zhao, P. Yang, N. Melosh, J. Feng, B. F. Chmelka, G. D. Stucky, *Adv. Mater.* **1998**, *10*, 1380.
- [14] P. Yang, D. Zhao, D. I. Margolese, B. F. Chmelka, G. D. Stucky, *Nature* **1998**, *396*, 152.
- [15] D. M. Antonelli, *Microporous Mesoporous Mater.* **1999**, *30*, 315.
- [16] D. Grosso, G. Soler-Illia, F. Babonneau, C. Sanchez, P. A. Albouy, A. Brunet-Bruneau, A. R. Balkenende, *Adv. Mater.* **2001**, *13*, 1085.
- [17] Y. K. Hwang, K. C. Lee, Y. U. Kwon, *Chem. Commun.* **2001**, 1738.
- [18] D. Khushalani, G. A. Ozin, A. Kuperman, *J. Mater. Chem.* **1999**, *9*, 1491.
- [19] G. Soler-Illia, A. Louis, C. Sanchez, *Chem. Mater.* **2002**, *14*, 750.
- [20] Y. Wang, S. Chen, X. Tang, O. Palchik, A. Zaban, Y. Koltypin, A. Gedanken, *J. Mater. Chem.* **2001**, *11*, 521.
- [21] P. Yang, D. Zhao, D. Margolese, B. F. Chemlka, G. D. Stucky, *Chem. Mater.* **1999**, *11*, 2813.
- [22] Y. Yue, Z. Gao, *Chem. Commun.* **2000**, 1755.
- [23] H. S. Yun, K. Miyazawa, H. S. Zhou, I. Honma, M. Kuwabara, *Adv. Mater.* **2001**, *13*, 1377.

- [24] P. Alberius-Henning, K. L. Frindell, R. C. Hayward, E. J. Kramer, G. D. Stucky, B. F. Chmelka, *Chem. Mater.* **2002**, *14*, 3284.
- [25] J. Wu, A. F. Gross, S. H. Tolbert, *J. Phys. Chem. B* **1999**, *103*, 2374.
- [26] T.-Q. Nguyen, J. Wu, V. Doan, B. J. Schwartz, S. Tolbert, *Science* **2000**, *288*, 652.
- [27] G. W. Heffner, D. S. Pearson, *Macromolecules* **1991**, *24*, 6295.
- [28] R. A. Vaia, H. Ishii, E. P. Giannelis, *Chem. Mater.* **1993**, *5*, 1694.
- [29] R. A. Vaia, E. P. Giannelis, *Macromolecules* **1997**, *30*, 8000.
- [30] C. Yang, F. P. Orfino, S. Holdcroft, *Macromolecules* **1996**, *29*, 6510.
- [31] W. R. Salaneck, O. Inganas, B. Themans, J. O. Nilsson, B. Sjogren, J.-E. Osterholm, J.-L. Bredas, S. Svensson, *J. Chem. Phys.* **1988**, *89*, 4613.
- [32] O. Inganas, W. R. Salaneck, J.-E. Osterholm, J. Laakso, *Synth. Met.* **1988**, *22*, 395.
- [33] C. Roux, M. Leclerc, *Macromolecules* **1992**, *25*, 2141.
- [34] O. K. Korovyanko, R. Osterbacka, X. M. Jiang, Z. V. Vardeny, R. A. J. Janssen, *Phys. Rev. B* **2001**, *64*, 235122.
- [35] N. C. Greenham, X. Peng, A. P. Alivisatos, *Phys. Rev. B* **1996**, *54*, 17628.
- [36] P. A. van Hal, M. P. T. Christiaans, M. M. Wienk, J. M. Kroon, R. A. J. Janssen, *J. Phys. Chem. B* **1999**, *103*, 4352.
- [37] T. J. Savenije, J. M. Warman, A. Goossens, *Chem. Phys. Lett.* **1998**, *287*, 148.